# Lewis Acid Adducts of Narrow Band Gap Conjugated Polymers

Gregory C. Welch and Guillermo C. Bazan*

Center for Polymers and Organic Solids, Department of Chemistry and Biochemistry, and Department of Materials, The University of California, Santa Barbara, California 93106, United States

S *Supporting Information*

ABSTRACT: We report on the interaction of Lewis acids with narrow band gap conjugated copolymers containing donor and acceptor units. Examination of the widely used poly[(4,4-bis(2-ethylhexyl)cyclopenta-[2,1-*b*:3,4-*b'*]dithiophene)-2,6-(diyl-alt-benzo[2,1,3]thiadiazole)-4,7-diyl] (**1**) shows weaker binding with $B(C_6F_5)_3$ when compared with a small molecule that contains a cyclopenta-[2,1-*b*:3,4-*b'*]dithiophene (CDT) unit

flanked by two benzo[2,1,3]thiadiazole (BT) fragments. Studies on model compounds representative of **1**, together with a comparison between $B(C_6F_5)_3$ and BBr_3, indicate that the propensity for Lewis acid coordination is decreased because of steric encumbrance surrounding the BT nitrogen sites. These observations led to the design of chromophores that incorporate an acceptor unit with a more basic nitrogen site, namely pyridal[2,1,3]thiadiazole (PT). That this strategy leads to a stronger B—N interaction was demonstrated through the examination of the reaction of $B(C_6F_5)_3$ with two small molecules bis(4,4-bis(hexyl)-4*H*-cyclopenta-[2,1-*b*:3,4-*b'*]dithiophene)-4,7-pyridal[2,1,3]thiadiazole (**8**) and bis{2-thienyl-(4,4-bis(hexyl)-4*H*-cyclopenta[2,1-*b*:3,4-*b'*]dithiophene)}-4,7-pyridal[2,1,3]thiadiazole (**9**) and two polymer systems (poly[(4,4-bis(2-ethylhexyl)cyclopenta-[2,1-*b*:3,4-*b'*]dithiophene)-2,6-diyl-alt-([1,2,5]thiadiazolo[3,4-*c*]pyridine)-4,7-diyl] (**10**) and poly[(4,4-bis(2-ethylhexyl)cyclopenta-[2,1-*b*:3,4-*b'*]dithiophene)-2,6-diyl-alt-(4',7'-bis(2-thienyl)-[1,2,5]thiadiazolo[3,4-*c*]pyridine)-5,5-diyl] (**11**). From a materials perspective, it is worth pointing out that through the binding of $B(C_6F_5)_3$, new NIR-absorbing polymers can be generated with band gaps from 1.31 to 0.89 eV. A combination of studies involving ultraviolet photoemission spectroscopy and density functional theory shows that the narrowing of the band gap upon borane coordination to the pyridal nitrogen on PT is a result of lowering the energies of *both* the highest occupied molecular orbital (HOMO) and lowest unoccupied molecular orbital (LUMO) of the optically relevant fragments; however, the LUMO is decreased to a greater extent, thereby giving rise to the narrowing of the gap.
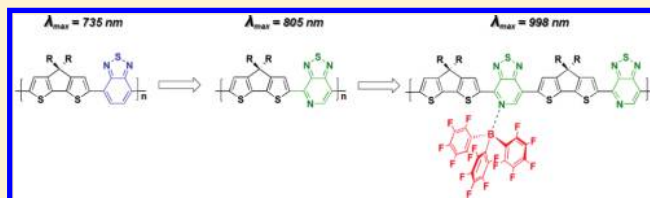
■ INTRODUCTION

Push—pull organic chromophores and related polymeric systems are an important class of semiconducting and light harvesting materials that have been studied and utilized in various technologies.[1] Their molecular structures contain electron rich and electron deficient moieties linked via a π-conjugated bridge. Photoexcitation leads to intramolecular charge-transfer from the electron rich fragment in the molecule, referred to as the donor (D), to the electron deficient segment, referred to as the acceptor (A).[2] Such a redistribution of electron density leads to absorption bands that can extend from the ultraviolet to well into the near-infrared regions of the spectrum, depending on the electronic offset between the donor and acceptor components and the overall delocalization length.[3—10] The resulting materials have found utility in many organic electronic and optical applications including use as nonlinear optics,[11—13] as light emitters for OLEDs,[14,15] as sensitizers in DSSCs[16—18] and more recently as light harvesting materials for bulk-heterojunction (BHJ) solar cells.[19] With respect to the latter, the incorporation of D/A conjugated copolymers with optical band gaps near 1.4 eV results in BHJ devices with excellent spectral overlap with the terrestrial solar spectrum and ultimately enables efficient photon harvesting and increased photocurrent generation.[20—22] Organic materials that absorb into the near-infrared (NIR) have also begun to

attract additional interest as they have potential to be incorporated into organic NIR photodetectors and NIR photovoltaic and electrochromic devices with the potential to outperform current inorganic counterparts.[23,24]

Due to the broad range of applications that take advantage of push—pull organic chromophores, there exists a demand for new strategies for designing materials with tunable optical and electronic properties. By far the most common method is to modify the electron donating or accepting character of the D or A fragments, respectively, by alteration of the molecular framework.[5,25—27] While this strategy has yielded many novel narrow band gap materials, the synthesis can often require multiple steps, and thus, new, general, and simpler approaches to modulate optical properties are desired. Methods such as protonation[28—35] or metal ion complexation[36—39] at basic sites, or chemical doping,[40,41] can greatly alter the optical and electronic properties of a material, although this can lead to charged species and loss of semiconducting behavior, respectively, traits that may impact device performance.

A wide range of conjugated polymers and related oligomers contain heteroatoms with available lone pairs of electrons.[20] Our

Scheme 1. Adduct Formation between 5,5′-Bis(benzo[2,1,3]thiadiazole)-3,3′-di-*n*-dodecylsilylene-2,2′-bithiophene (BT/DTS/BT) and B(C$_6$F$_5$)$_3$ as Described in Reference 42
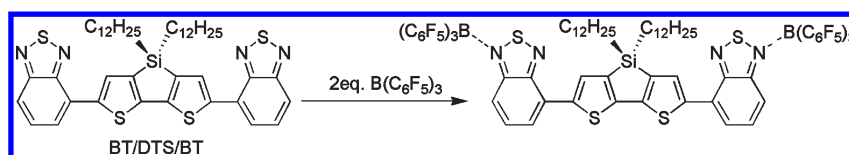
group recently demonstrated that through the selective binding of Lewis acids to an accessible nitrogen atom on the acceptor unit, electron density can be removed from the π-conjugated system, resulting in a narrowing of the band gap.[42] In the case of 5,5′-bis(benzo[2,1,3]thiadiazole)-3,3′-di-*n*-dodecylsilylene-2,2′-bithiophene (BT/DTS/BT), shown in Scheme 1, one observes a change in the absorption maximum (λ_{max}) from ~500 to ~650 nm upon binding of B(C$_6$F$_5$)$_3$ to the nitrogen atoms in the outer two benzo[2,1,3]thiadiazole (BT) units. The degree of change in the absorption properties can be tuned by varying the strength of the Lewis acid, with the strongest Lewis acid leading to the smallest band gap, i.e., most red-shifted absorption spectrum. Recent reports have demonstrated a similar phenomenon for benzo[1,2-*c*:4,5-*c′*]bis([1,2,5]thiadiazole) (BBTD)[25] and thiazolyl[43] based π-conjugated organic systems. We therefore envisioned extending this methodology to related polymeric derivatives, with a focus on B(C$_6$F$_5$)$_3$. This Lewis acid has found applications in various fields of chemistry owing to its strong acidity (comparable to BF$_3$ and BCl$_3$), resistance to B−C bond cleavage, and tolerance to air and moisture.[44−46] For example, B(C$_6$F$_5$)$_3$ has been widely used as cocatalyst in the polymerization of olefins,[47] a primary catalyst for organic transformations,[48] and, more recently, as a key component for metal-free catalysis via frustrated Lewis pairs.[49−51] Herein we examine the interaction of B(C$_6$F$_5$)$_3$ with D/A conjugated polymers to untangle electronic and steric contributions to the binding equilibrium and modification of optical properties. Furthermore, we report on the development of a new class of materials incorporating a pyridal-like nitrogen into the π-conjugated backbone to increase the propensity toward Lewis adduct formation.

■ RESULTS AND DISCUSSION

Addition of Lewis Acids to Polymer 1 and Related Small Molecules. Initial efforts centered on studying the reaction between poly[(4,4-bis(2-ethylhexyl)cyclopenta-[2,1-b:3,4-b′]-dithiophene)-2,6-(diyl-alt-benzo[2,1,3]thiadiazole)-4,7-diyl] (**1** in Figure 1)[52−54] and B(C$_6$F$_5$)$_3$. This polymer has been previously used in the fabrication of BHJ solar cells with power conversion efficiencies near 5.5% and is a structural analogue to BT/DTS/BT, except for the C-based cyclopentadithienyl framework and the use of 2-ethylhexyl substituents.[52,55] Addition of 1 equiv of B(C$_6$F$_5$)$_3$ to a green *o*-dichlorobenzene (*o*-DCB) solution of **1** results in no visible reaction or observable color change. On the basis of our previous findings,[42] a solution color change would imply the formation of a new absorbing species in solution. Analysis by UV−vis−NIR spectroscopy reveals a decrease of the band centered at 780 nm and the appearance of a weak and broad low energy transition in the 900−1700 nm range (Figure 2a). Addition of up to 5 equiv B(C$_6$F$_5$)$_3$ resulted in no further significant change in the absorption spectra, with features attributed to **1** still present. Exposure of these solutions to
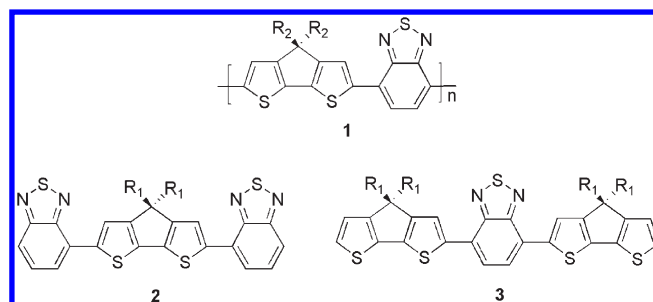

Figure 1. Structures of cyclopentadithiopene-*co*-benzothiadiazole co-polymer **1** and related small molecules **2** and **3**. R$_2$ = 2-ethylhexyl, R$_1$ = hexyl.

pyridine (Py) regenerates the original absorption spectrum of **1**, which we attribute to formation of the Py−B(C$_6$F$_5$)$_3$ adduct[56] and the release of the parent polymer. These data should be compared against the situation with BT/DTS/BT which can bind 2 equiv of B(C$_6$F$_5$)$_3$ under similar experimental conditions. Our initial thoughts centered on the possibility that the difference in reactivity could be attributed to the more sterically hindered BT nitrogen atoms, which are doubly flanked in **1** vis a vis BT/DTS/BT.

To probe the role of steric hindrance, we employed the smaller Lewis acid BBr$_3$. Addition of 1 equiv of BBr$_3$ to an *o*-DCB solution of **1** resulted in an immediate color change from green to faint yellow-green, while addition of 5 equiv gave a yellow-red solution. The absorption spectra of these solutions (Figure 2b) display complete disappearance of the absorption band due to the parent polymer **1** and the emergence of broad bands with $\lambda_{max} \sim 1160$ nm and absorption onsets (λ_{onset}) extending beyond 2000 nm. Such spectra are reminiscent of doped polymers.[8] However, addition of excess Py leads to removal of BBr$_3$ and a return to the absorbance spectrum of **1**. These transformations are consistent with the borane forming a Lewis adduct via a dative interaction with a heteroatom on the main chain.[25,42] Unfortunately, all attempts to isolate and fully characterize **1**/BBr$_3$ adducts proved unsuccessful due to decomposition to unidentified products upon standing in solution for several hours or when efforts were made to form films via spin coating techniques. We attribute this instability to the reactivity of the B−Br bond when the boron atom is bound to a Lewis base.

In order to understand the results obtained with **1**, we synthesized, examined, and compared the reactivity of two related well-defined molecules, namely 5,5′-bis(benzo[2,1,3]-thiadiazole)-4,4-bis(hexyl)-4*H*-cyclopenta[2,1-*b*;3,4-*b′*]-dithiophene (**2**) and bis(4,4-bis(hexyl)-4*H*-cyclopenta[2,1-*b*;3,4-*b′*]-dithiophene)}-4,7-benzo[2,1,3]thiadiazole (**3**). Compounds **2** and **3**, shown in Figure 1, contain the same structural units as in **1** and were synthesized by adapting literature procedures;[3,42] complete details can be found in the Supporting Information.
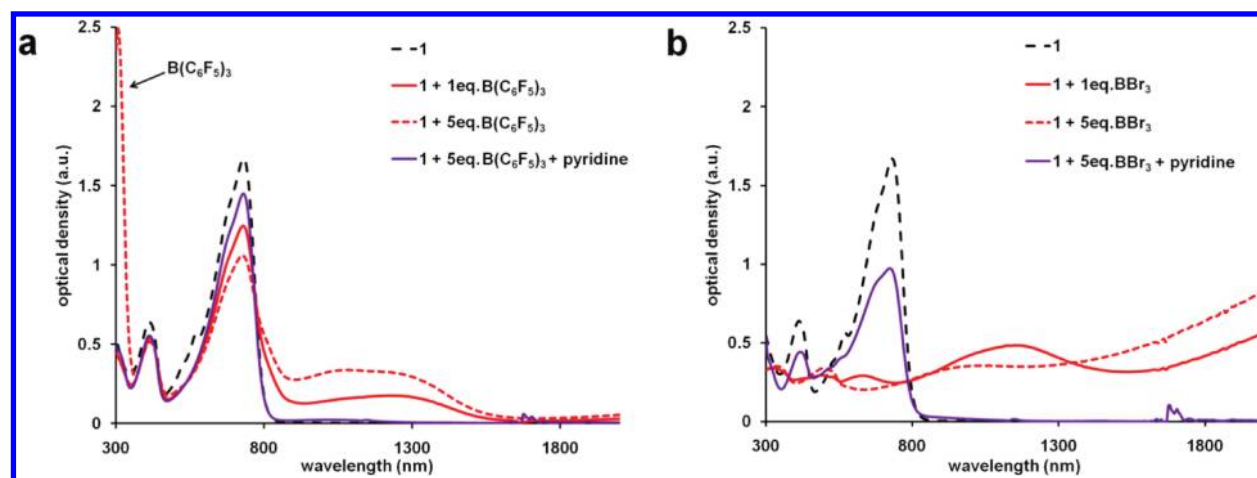
B

dx.doi.org/10.1021/ja110968m |*J. Am. Chem. Soc.* XXXX, XXX, 000–000

Figure 2. UV−vis−NIR absorption spectra of **1** with varying equivalents of $B(C_6F_5)_3$ (a) and BBr_3 (b) in o-DCB solution at room temperature.
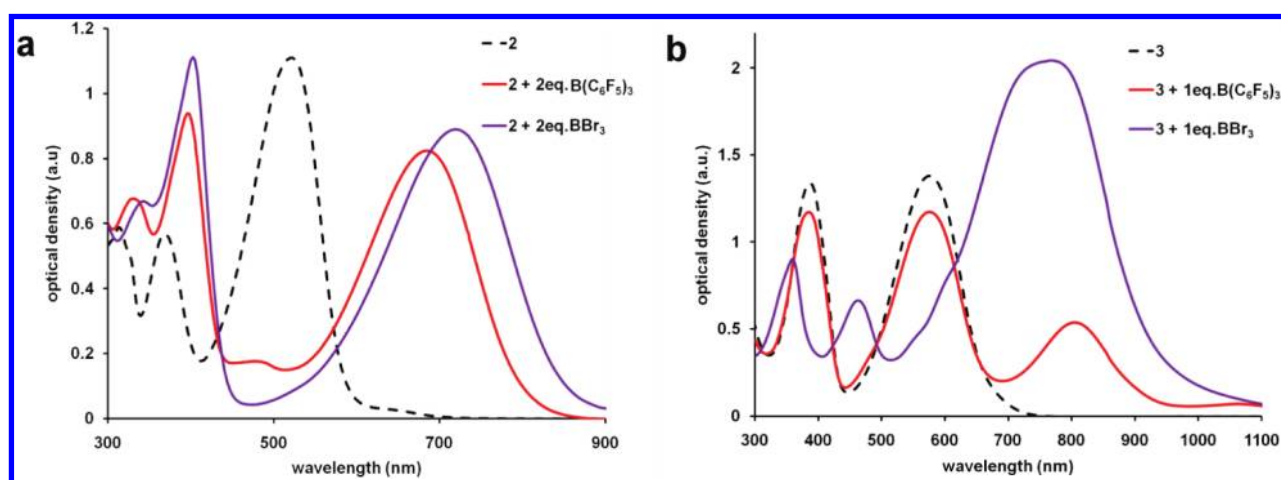

Figure 3. UV−vis−NIR absorption spectra of the small molecules **2** (a) and **3** (b) with no added Lewis acid (black), 1 equiv of $B(C_6F_5)_3$ per BT unit (red), and 1 equiv of BBr_3 per BT unit (purple) in o-DCB solution at room temperature.

For **3**, the BT nitrogen atoms exist in the same chemical environment as in **1**, as they are flanked by cyclopenta-[2,1-b:3,4-b']dithiophene (CDT) donor units, whereas the two BT nitrogen atoms of **2** exist in different chemical environments: one is flanked by a CDT unit while the other is located at the open terminus of the molecule. The difference in accessibility of each nitrogen atom was anticipated to provide insight into the reactivity toward 3-coordinate boranes.

Addition of 2 mol equiv of $B(C_6F_5)_3$ to **2** in o-DCB (i.e., one boron center per BT unit) results in a color change from red to blue. As shown by the UV−vis−NIR spectra in Figure 3a, there is a complete disappearance of the absorption band at λ_{max} = 518 nm with the concomitant emergence of a new band with λ_{max} = 686 nm, attributed to the bis-$B(C_6F_5)_3$ adduct.[42] This complexation is illustrated in Scheme 2. Similarly, addition of 2 mol equiv of the stronger and smaller Lewis acid BBr_3 to **2** leads to an absorption band with λ_{max} = 717 nm, which is further red-shifted relative to what is observed with $B(C_6F_5)_3$. These trends and observations are similar to those previously obtained with BT/DTS/BT; adduct formation is nearly complete with 2 equiv borane, and the stronger Lewis acid BBr_3 gives rise to the furthest narrowing of the optical transition.[42]

In contrast to the observations for **2**, there is no observable color change by visual inspection of **3** in o-DCB upon addition of

1 mol equiv $B(C_6F_5)_3$ (i.e., one boron center per BT unit). The absorption spectra of this mixture shown in Figure 3b displays a slight decrease of the intensity in the bands at 378 and 568 nm, and the appearance of a weak band at λ_{max} = 810 nm, which is likely due to Lewis adduct formation.[44] Since it is reasonable that the basicity of the BT nitrogens in **2** and **3** should not greatly differ, the difference in the spectral characteristics in Figure 3a,b suggests that steric interference is pronounced in the case of **3**; thus, the equilibrium favors free borane and chromophore, as shown in Scheme 2. Increasing the concentration of $B(C_6F_5)_3$ in solution to upward of 5 mol equiv results in near complete disappearance of the UV−vis spectra features of **3** and an increase in the intensity of the long wavelength transition, see Supporting Information. This result implies that B−N adduct formation is possible, but not as favored as observed with **2**. We thus examined the addition of BBr_3, which leads to an immediate solution color change from violet to yellow-green. The absorption spectrum provides more detail; most notably the change-transfer absorption band is red-shifted by 207 nm, as shown in Figure 3b, and is considerably broadened. More detailed characterization of the **3**−BBr_3 interaction could not be achieved due to the instability of the product. Thus, we initially conclude that while the absorption spectra of BT containing chromophores can be altered upon Lewis acid addition, steric constraints are more

Scheme 2. Reactions of 2 and 3 with B(C$_6$F$_5$)$_3$ at Room Temperature in *o*-DCB[a]
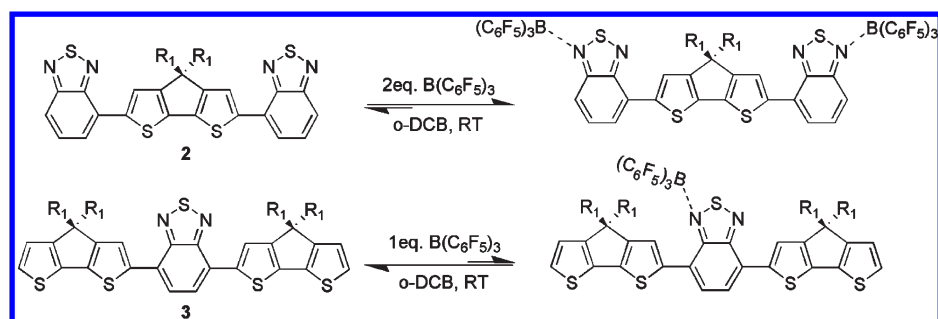
[a] B(C$_6$F$_5$)$_3$ forms a strong adduct with the external N-atoms of the BT unit in **2**. Less pronounced adduct formation is observed with the internal BT N-atom of **3**. R$_1$ = hexyl.

Scheme 3. Incorporation of a Pyridal Nitrogen into the Core D/A Backbone of the Organic Materials via Incorporation of a PT Fragment[a]
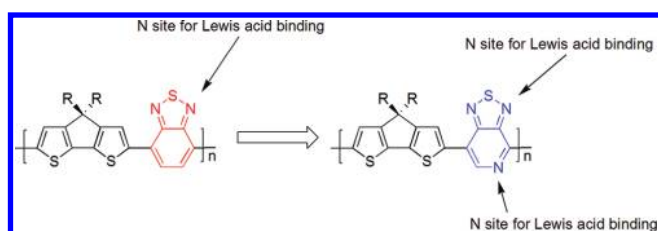
[a] It is hypothesized that the pyridal N-atom has a higher basicity and is more sterically accessible than the azole N-atom, allowing for stronger interactions with organoboranes.

pronounced when BT is flanked by two CDT units, as in the situation with **1**. Subsequent efforts were therefore focused on the development of new π-conjugated small molecules and polymers that would more strongly bind B(C$_6$F$_5$)$_3$.

Design and Synthesis of Conjugated Polymers and Small Molecules Containing the Pyridalthiadiazole (PT) Acceptor Unit. On the basis of the known affinity of B(C$_6$F$_5$)$_3$ to bind to pyridine[13,56,57] we turned our attention to the [1,2,5]-thiadiazolo[3,4-c]pyridine (PT) acceptor subunit, as shown in Scheme 3.[26,58] The PT unit is a strong electron acceptor[26] which can lead to charge-transfer characteristics when coupled with complementary donor fragments. Very recently, thiophene-based copolymers incorporating the PT unit have been reported as effective narrow band gap materials for high performance BHJ solar cells.[59] Furthermore, PT offers a pyridal N-atom for possible Lewis acid binding, which is more basic and accessible than the BT counterpart (Scheme 3). These considerations led us to the design of four novel polymers and model compounds as shown in Scheme 4. The polymer poly[(4,4-bis(2-ethylhexyl)-cyclopenta-[2,1-*b*:3,4-*b′*]dithiophene)-2,6-diyl-alt-([1,2,5]-thiadiazolo[3,4-*c*]pyridine)-4,7-diyl] (**10**) incorporates the CDT unit as the donor moiety and the PT unit as the acceptor moiety. A polymer structure with thiophene spacers between the CDT and PT units, namely poly[(4,4-bis(2-ethylhexyl)cyclopenta-[2,1-*b*:3,4-*b′*]dithiophene)-2,6-diyl-alt-(4′,7′-bis(2-thienyl)-[1,2,5]-thiadiazolo[3,4-*c*]pyridine)-5,5-diyl] (**11**), was targeted to explore more subtle steric and electronic effects. The two small molecules bis(4,4-bis(hexyl)-4*H*-cyclopenta[2,1-*b*:3,4-*b′*]dithiophene)-4,7-pyridal[2,1,3]thiadiazole (**8**) and bis{2-thienyl-(4,4-bis(hexyl)-4*H*-cyclopenta[2,1-*b*:3,4-*b′*]dithiophene)}-4,7-pyridal-

[2,1,3]thiadiazole (**9**) are related to **10** and **11**, respectively, and provide well-defined species to enable more detailed characterization via NMR spectroscopy. All four novel materials exhibit unique properties in their own right and for this reason are described in some detail below.

The synthesis of small molecules **8** and **9** is outlined in Scheme 4. The commercially available precursor 4,7-dibromo-pyridal[2,1,3]thiadiazole (**6**) was used as received, while 4,7-bis(5-bromo-2-thienyl)[1,2,5]thiadiazolo[3,4-*c*]pyridine (**7**) and the stannylated compounds 5-(trimethylstannyl)-4,4-bis(hexyl)-4*H*-cyclopenta[2,1-*b*;3,4-*b′*]dithiophene (**4**) and 4,4-bis(2-ethylhexyl)-2,6-bis(trimethylstannyl)-4*H*-cyclopenta[2,1-*b*:3,4-*b′*]-dithiophene (**5**) were synthesized and purified according to literature procedures.[3,26] Full experimental details and spectroscopic characterization can be found in the Supporting Information. The targets **8** and **9** were obtained as purple solids via reaction of 2 equiv of **4** with 1 equiv of **6** or **7**, respectively, in yields greater than 70%. These compounds exhibit good solubility in most organic solvents and were structurally characterized by elemental analysis, multinuclear NMR solution spectroscopy, and mass spectrometry. In comparison to the related BT small molecules **2** and **3** described above, species **8** and **9** exhibit asymmetric π-conjugated organic structures, resulting in chemically distinct NMR spectra for the aromatic component. For example, compound **8** exhibits seven aromatic resonances in the ^{1}H NMR spectrum, indicating all aromatic protons exist in chemically different environments. The asymmetry is also observed in the ^{13}C NMR spectrum, where two inequivalent CDT bridging carbon atoms can be identified. Neither **8** nor **9** showed obvious thermal transitions in the 0−250 °C range in the solid state, as determined using differential scanning calorimetery (DSC).

Polymers **10** and **11** were synthesized via a microwave assisted Stille polymerization procedure, as shown in Scheme 4.[52] Both polymers incorporate 2-ethylhexyl side chains on the donor CDT unit to promote good solubility in organic media, particularly chlorobenzene (CB) and *o*-DCB (~10 mg per mL). The average number molecular weights were determined by gel permeation chromatography (GPC) at 150 °C in 1,2,5-trichlorobenzene, and were found to be 16 and 18 kg mol^{-1} for **10** and **11**, respectively. The polydispersity index (PDI) of each polymer was approximately 2. Due to the nature of the step-growth polymerization, it is likely that each polymer exhibits a regioirregular structure.[26] No thermal transitions in the solid state were detected by DSC in the 0−250 °C range.

Scheme 4. Synthesis of Small Molecules 8 and 9 and Polymers 10 and 11[a]
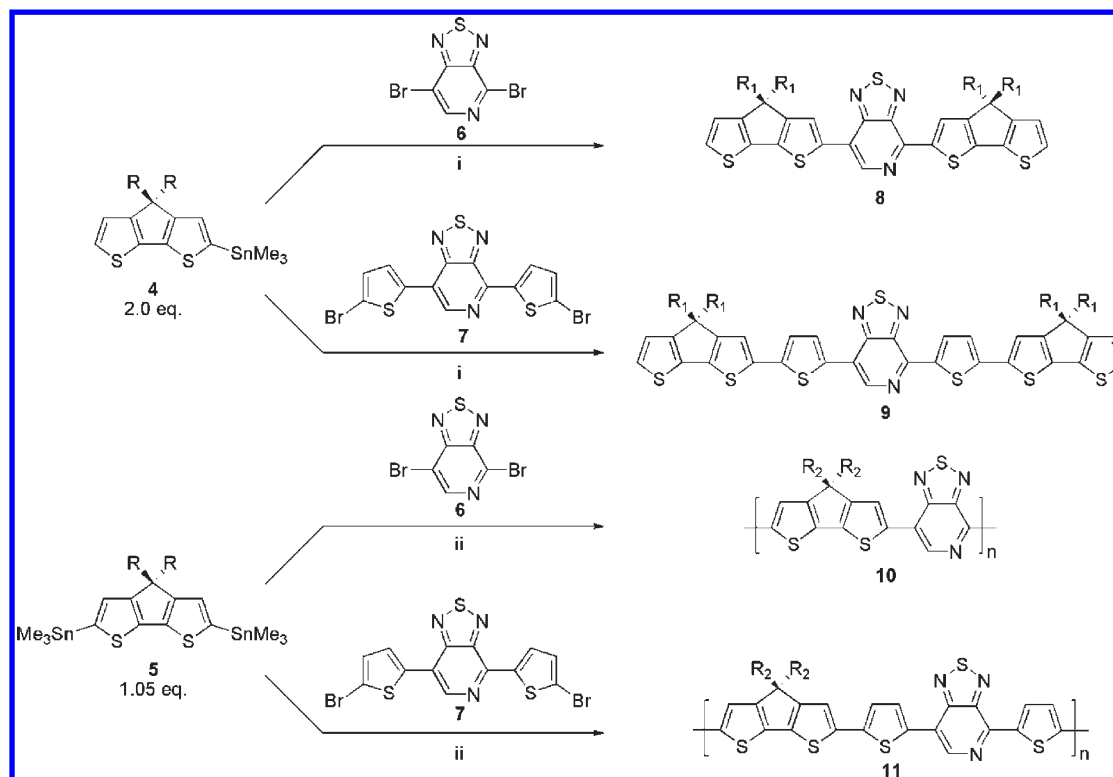
[a] (i) Microwave irradiation, 170 °C, 5 mol % Pd(PPh$_3$)$_4$, toluene; (ii) microwave irradiation, 200 °C, 5 mol % Pd(PPh$_3$)$_4$, xylenes. R$_1$ = hexyl, R$_2$ = 2-ethylhexyl.
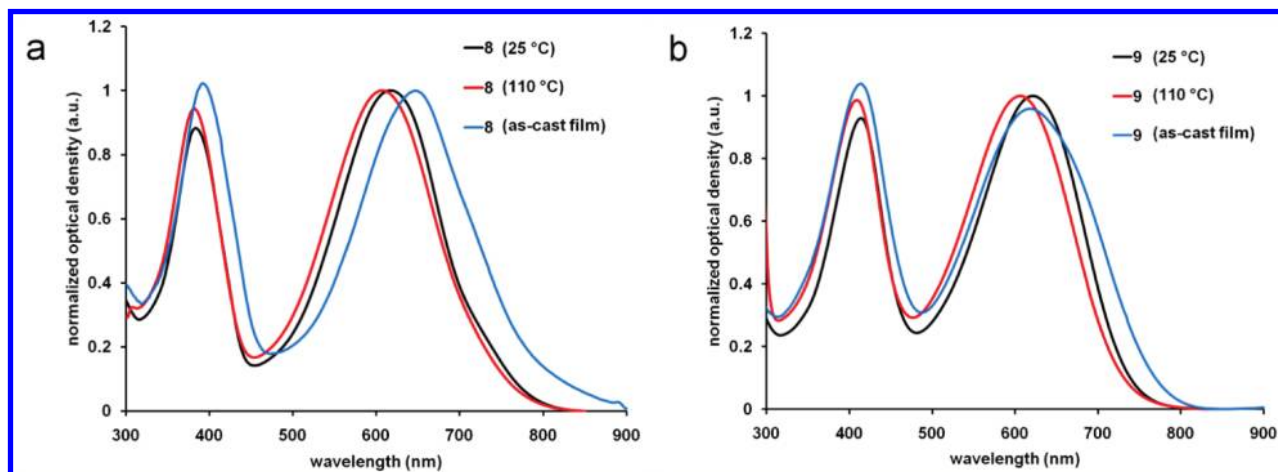

Figure 4. Normalized UV−vis−NIR absorption spectra for small molecules 8 (a) and 9 (b). Solution spectra at 25 °C (black) and 110 °C (red) recorded in *o*-DCB. As-cast film spectra on quartz (blue) obtained at 25 °C.

Optical Absorption Properties of 8 and 9. Absorption characteristics of **8** and **9** were determined to provide a baseline measure when we examine the effect of adding Lewis acids to them and their polymeric counterparts. The normalized UV−vis−NIR absorption spectra of **8** and **9** are shown in Figure 4, and all the relevant data are summarized in Table 1. The λ_{max} values in *o*-DCB at 25 °C for the low energy transitions of **8** and **9** occur at 618 and 626 nm, respectively. Heating these solutions to 110 °C using a temperature controlled heating stage (see Supporting Information) has little effect on the spectral characteristics, and implies that there is negligible interchromo-phore aggregation under these conditions.[52] Transitioning from solution to thin film, the λ_{max} of **8** red shifts 28 nm while that of **9** remains mostly unchanged. However, the λ_{onset} values for **8** and **9** are red-shifted 26 and 28 nm, respectively. The optical band gaps of **8** and **9**, determined from the onset of the thin film absorption, were estimated to be 1.57 and 1.61 eV, respectively. These similar values suggest the increased π-conjugated length afforded by the two additional thiophene units in **9** offsets any significant LUMO level destabilization caused by their ability to

Table 1. Summary of Optical Data of Small Molecules and Polymers

compound	$\lambda_{max}{}^a$ (nm) (ε_{max} [M^{-1} cm^{-1}])	$\lambda_{onset}{}^a$ (nm)	$\lambda_{max}{}^b$ (nm)	$\lambda_{onset}{}^b$ (nm)	band gap^c (eV)
8	618 (35 440)	766	646	790	1.57
	386 (30 670)		390		
9	626 (37 500)	742	626	768	1.61
	418 (30 520)		416		
10	805 (44 980)^d	890	830	944	1.31
	420 (15 410)^d		412		
11	680 (38 120)^d	855	690	875	1.42
	450 (22 450)^d		452		

^{a} Solution (o-DCB). ^{b} Film (quartz). ^{c} Estimated from onset of film absorption. ^{d} Approximate polymer extinction coefficient determined using molecular weight of repeat unit.
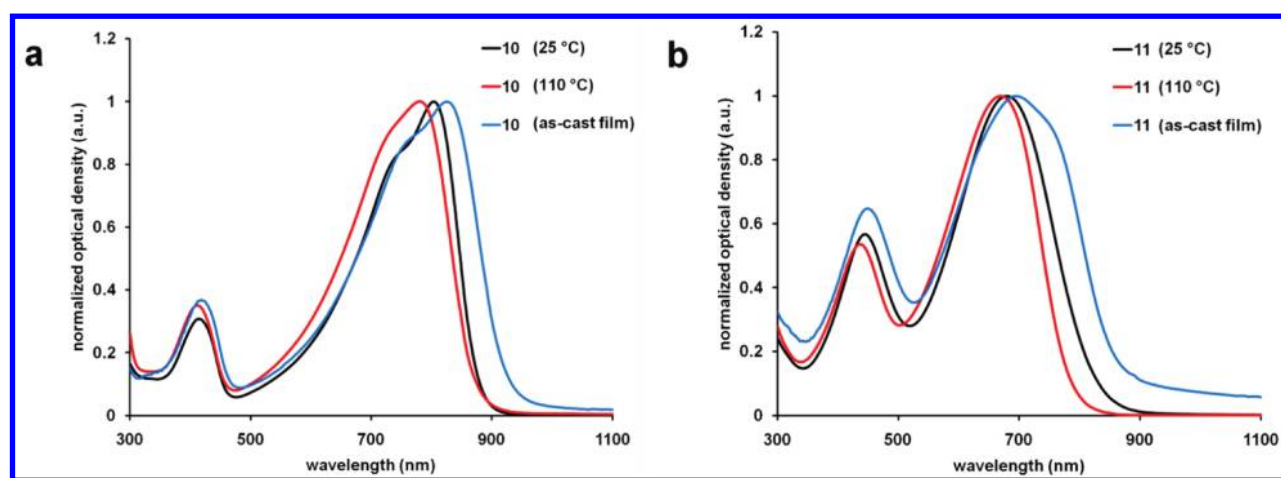

Figure 5. Normalized UV−vis−NIR absorption spectra for polymers **10** (a) and **11** (b). Solution spectra at 25 °C (black) and 110 °C (red) recorded in o-DCB. As-cast film spectra on quartz (blue) obtained at 25 °C.

inductively donate electron density.[60] It is also worth pointing out that **8** has a smaller band gap than the corresponding BT-containing analogues (1.87−1.95 eV),[3] but is comparable to DAD small molecules based upon the thienopyrazine acceptor unit (1.55−1.55 eV),[3] thus demonstrating the high electron affinity of the PT unit.

Optical Absorption Properties of 10 and 11. The absorption spectra of polymers **10** and **11** in o-DCB solution at 25 and 110 °C, and as thin films, are shown in Figure 5, with full details listed in Table 1. The λ_{max} values of **10** and **11**, at 25 °C in o-DCB, are 805 and 680 nm, respectively. Polymer **10** exhibits a broad absorption spectrum with an estimated λ_{onset} in solution of 890 nm. Polymer **11** is blue-shifted relative to **10** with an λ_{onset} = 855 nm in solution at 25 °C. The introduction of thiophene linkages[61] between the CDT donor unit and the PT acceptor unit has the primary effect of destabilizing the LUMO energy level (vide infra), resulting in a widening of the band gap, and thus the blue-shifted absorption spectra of **11** versus **10**. The optical absorption of polymers **10** and **11** shows a dependence on solution temperature, as heating to 110 °C results in a slight blue shift of the low energy absorption band. This result is consistent with aggregation of the polymer chains in solution.[52] A transition from solution to film results in red-shifted absorption spectra for both **10** and **11**. The optical band gaps of **10** and **11** in the solid state were estimated to be 1.31 and 1.42 eV, respectively. Compared to the related BT derivatives,[4,52] polymers **10**

and **11** have absorption spectra that are significantly red-shifted due to the higher electron affinity of the PT unit.

Reaction of B(C_6F_5)$_3$ with 8 or 9. A slight color change from blue to blue-green is observed upon addition of 1 equiv B(C_6F_5)$_3$ to **8** in o-DCB. Analysis by UV−vis spectroscopy at 25 °C reveals a large red shift in λ_{max} (Δ = 136 nm) and λ_{onset} (Δ = 26 nm), as shown in Figure 6a. These are hallmarks of B(C_6F_5)$_3$ adduct formation, and based on the lack of reactivity with **3** discussed above, we presume that binding occurs via the pyridal N-atom, as depicted in Scheme 5.[3,62] Figure 6a also exhibits a shoulder at approximately 615 nm, due to the presence of unreacted **8**. This observation implies that equilibrium exists between free and coordinated **8** at 25 °C in solution. Transitioning from solution to the solid state, equilibrium is driven toward adduct formation, and the absorption spectrum only exhibits features from the **8**−B(C_6F_5)$_3$ adduct. Comparatively, addition of greater than 1 equiv of Lewis acid to **8** in solution shifts the equilibrium in favor of adduct formation, as determined by UV−vis spectroscopy, see Supporting Information. Upon addition of Py, the borane is displaced from **8**. Parent **8** can be recovered by solvent removal and separation from the (C_6F_5)$_3$B−Py adduct by flash column chromatography with hexanes. Adduct formation is therefore chemically reversible.

In an analogous fashion to **8**, small molecule **9** was subjected to the addition of 1 equiv of B(C_6F_5)$_3$. The resulting solution and film absorption spectra are shown in Figure 6b. Red shifts of
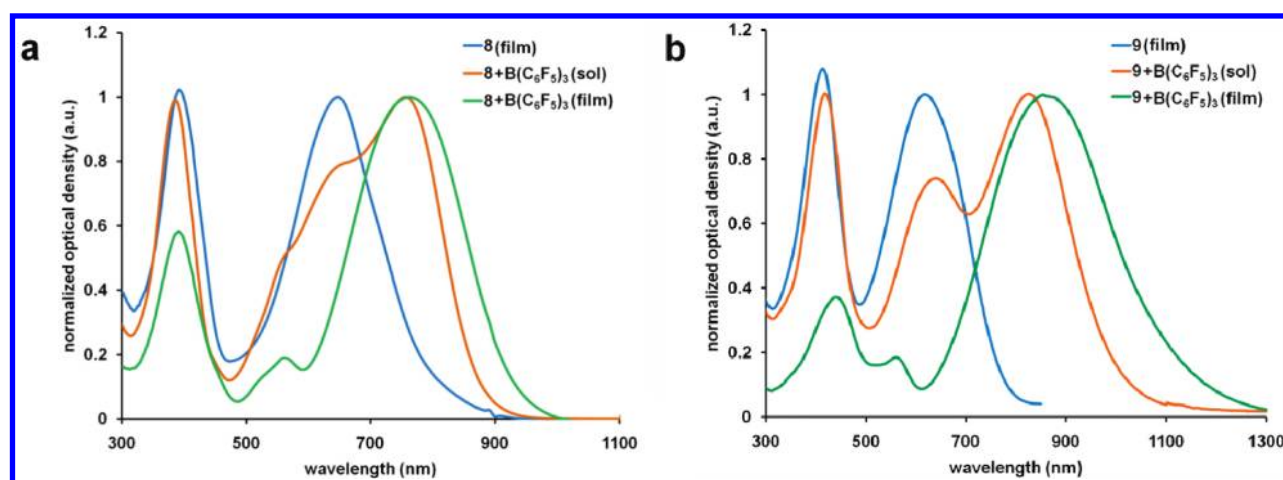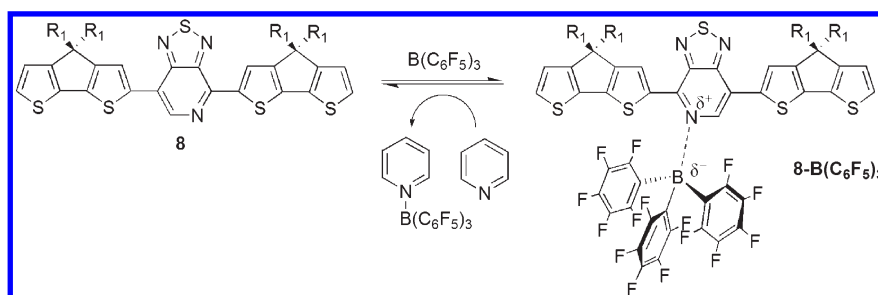
Figure 6. Normalized UV−vis−NIR absorption spectra of (a) **8** as-cast thin film (blue), **8** + 1 equiv $B(C_6F_5)_3$ in *o*-DCB solution (orange) and as-cast thin film (green); (b) **9** as-cast thin film (blue), **9** + 1 equiv $B(C_6F_5)_3$ in *o*-DCB solution (orange) and as-cast thin film (green).

Scheme 5. Proposed Adduct Formation between 8 and $B(C_6F_5)_3$[a]

[a] Adduct formation is fully reversible in the presence of Py. R1 = hexyl.

Table 2. Summary of Optical Data of Small Molecule and Polymer Lewis Adducts with $B(C_6F_5)_3$

compound	λ_{max}[a] (nm)	λ_{onset}[a] (nm)	λ_{max}[b] (nm)	λ_{onset}[b] (nm)	band gap[c] (eV)
8−$B(C_6F_5)_3$	752	892	764	950	1.31
	562, 640, 384		558, 386		
9−$B(C_6F_5)_3$	820	1022	868	1152	1.08
	632, 416		568, 444		
10−$B(C_6F_5)_3$	998	1162	1050	1290	0.96
	440		410		
11−$B(C_6F_5)_3$	986	1236	1090, 480	1395	0.89
	450				

[a] Solution (*o*-DCB). [b] Film (quartz). [c] Determined from λ_{onset}.

194 and 280 nm for λ_{max} and λ_{onset}, respectively, were observed in solution. Again, in solution, an equilibrium exists between free and bound borane, and upon transitioning to the solid state, only the **9**−$B(C_6F_5)_3$ adduct is observed. The optical band gap in the solid state of the adduct **9**−$B(C_6F_5)_3$ was determined to be 1.08 eV (Table 2).

Further insight into the reaction of **8** and **9** with $B(C_6F_5)_3$ was obtained by using multinuclear NMR solution spectroscopy. The ^{1}H NMR spectrum of an equal molar solution of **8** and $B(C_6F_5)_3$ in CD_2Cl_2 revealed significant broadening of the aromatic proton resonances at 300 K (Figure 7). This observation indicates that an exchange mechanism exists between **8** and possibly the **8**−$B(C_6F_5)_3$ adduct that is commensurate with the NMR time scale.

Upon cooling to 280 K the aromatic resonances sharpen, revealing resonances attributable to **8** and a new species, assigned to **8**−$B(C_6F_5)_3$. Further cooling to 230 K shifts the equilibrium toward adduct formation, and thus, only signals from **8**−$B(C_6F_5)_3$ can be observed. The equilibrium constant at 280 K was determined to be 1.2×10^2 M^{-1}. For reference, no significant change in the ^{1}H NMR spectrum of **8** was observed upon cooling from 300 to 230 K, see Supporting Information. A similar equilibrium between $B(C_6F_5)_3$ and lutidine has recently been observed and characterized.[63,64] The ^{19}F NMR spectrum at 300 K shown in Figure 8 displays 3 major resonances at −128.2, −143.8, and −160.9, for the *ortho*, *meta*, and *para* resonances of free $B(C_6F_5)_3$, respectively, consistent with an equilibrium
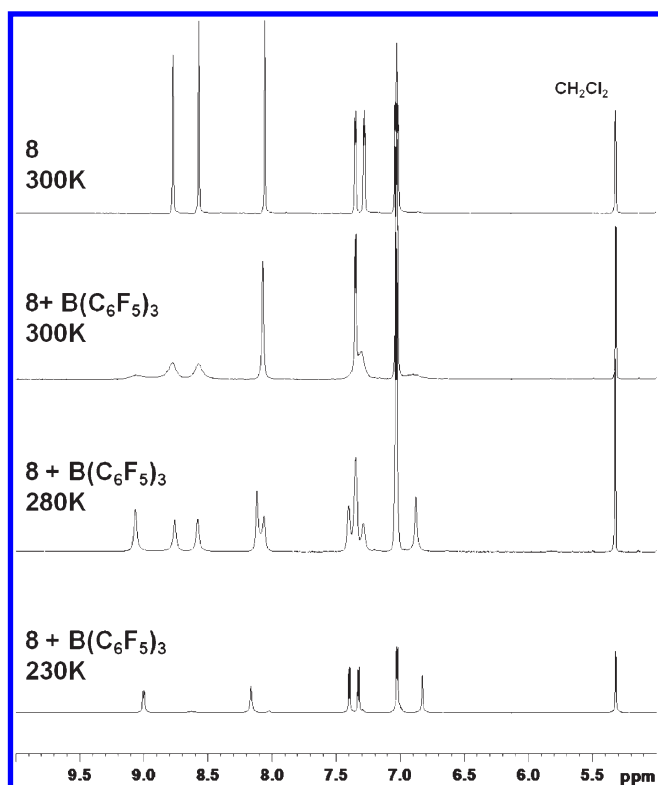
G

dx.doi.org/10.1021/ja110968m |*J. Am. Chem. Soc.* XXXX, XXX, 000–000

Figure 7. Aromatic region of the ^{1}H NMR spectra of **8** (top) and **8** + 1 equiv B(C$_6$F$_5$)$_3$ at various temperatures from 300 to 230 K. All spectra were recorded in CD$_2$Cl$_2$. Upon addition of B(C$_6$F$_5$)$_3$ the aromatic resonances of **8** are broadened due to rapid exchange of bound and unbound Lewis acid. Upon cooling to 280 K, resonances for **8** and **8**–B(C$_6$F$_5$)$_3$ are observed. Further cooling to 230 K drives the equilibrium fully toward adduct formation and resonances for **8**–B(C$_6$F$_5$)$_3$ are exclusively observed.

Figure 8. ^{19}F NMR spectra of B(C$_6$F$_5$)$_3$ (top) and B(C$_6$F$_5$)$_3$ + 1 equiv of **8** at various temperatures from 300 to 230 K. All spectra were recorded in CD$_2$Cl$_2$. Upon cooling the reaction mixture from 300 to 230 K, adduct formation is observed as indicated by the disappearance of the resonances for free B(C$_6$F$_5$)$_3$ and the appearance of 15 inequivalent fluorine resonances for four coordinate boron with restricted motion.

mixture that favors the unbound starting materials. Upon cooling to 230 K, the three *ortho*, *meta*, and *para* resonances of free B(C$_6$F$_5$)$_3$ disappear, and 15 new resonances from −125 to −166 ppm are observed which indicates that all the fluorines in B(C$_6$F$_5$)$_3$ are inequivalent and is consistent with formation of **8**–B(C$_6$F$_5$)$_3$, in which the boron center exists in a 4-coordinate pseudotetrahedral orientation.[42,44,57] Steric interactions between the C$_6$F$_5$ rings and either the hexyl alkyl chains or the thiophene rings restrict rotation about the B−N and B−C bonds, thus rendering all 15 fluorine atoms inequivalent. Addition of an equal molar amount of pyridine to this solution results in regeneration of **8** and the Py-B(C$_6$F$_5$)$_3$ adduct. A similar equilibrium was observed in CD$_2$Cl$_2$ by ^{1}H and ^{19}F NMR spectroscopy for an equal molar mixture of **9** and B(C$_6$F$_5$)$_3$. Here, the equilibrium constant at 280 K was determined to be 2.8 × 10^2 M^{-1}. The slightly stronger affinity of **9** compared to **8** for binding of B(C$_6$F$_5$)$_3$ is likely attributed to (i) a more accessible pyridal N-atom due to a diminished steric impact from the CDT alkyl substituents, and (ii) an increased basicity at the pyridal N-atom due to the inductively donating effect of the additional thiophene linkages. The B(C$_6$F$_5$)$_3$ adducts of **8** and **9** are sensitive to H$_2$O and readily hydrolyze to yield pyridinum borate salts, a known decomposition pathway for nitrogen-based B(C$_6$F$_5$)$_3$ adducts.[65,66] It is also worth mentioning that while the S atoms of **8** and **9** have available lone pairs of electrons for potentially binding of Lewis bases, previous work has demonstrated that
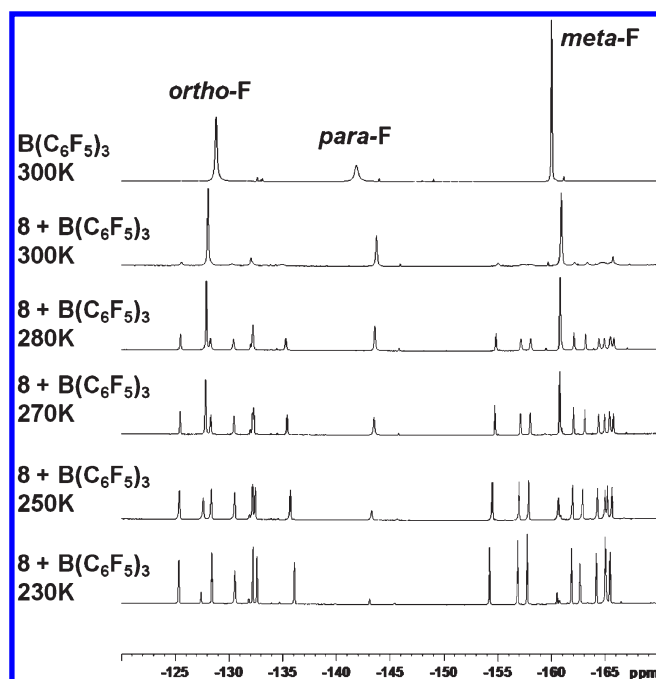
B(C$_6$F$_5$)$_3$ has a stronger propensity to form adducts with harder N-containing bases.[42] As an aside, we investigated the related and sterically less hindered molecule 2,2′-bithiophene, which contains no N-atoms, and observed no evidence of adduct formation with B(C$_6$F$_5$)$_3$ via ^{1}H and ^{19}F NMR solution spectroscopy at 300 K (see Supporting Information). We therefore conclude that any interaction of B(C$_6$F$_5$)$_3$ with the S atoms of **8** or **9** is highly unlikely.

Reaction of B(C$_6$F$_5$)$_3$ with Polymers 10 and 11. In *o*-DCB solution, **10** was subjected to the addition of varying equivalents of B(C$_6$F$_5$)$_3$, and the resulting absorption spectra are provided in Figure 9a. Upon addition of 0.1 equiv B(C$_6$F$_5$)$_3$ the absorption peak at ~805 nm decreases, while a new red-shifted absorption peak appears at ~980 nm. Addition of 0.5 equiv of B(C$_6$F$_5$)$_3$ results in almost complete disappearance of the absorption band for **10**, and an increase in the strength of the low energy band. Further addition of B(C$_6$F$_5$)$_3$, up to 10 equiv, results in a progressive red shift of λ$_{max}$ (980 to 1000 nm), while the λ$_{onset}$ is only slightly red-shifted. This observation can likely be attributed to equilibrium existing between free and bound **10** in solution. Increasing the concentration of B(C$_6$F$_5$)$_3$ in solution shifts the equilibrium in favor of adduct formation. These observations are in stark contrast to the reaction of **1** and B(C$_6$F$_5$)$_3$, where complete quenching of the absorption of **1** is not observed upon addition of excess Lewis acid (Figure 2a).

Given the electronic communication along the backbone of a conjugated polymer, it seemed reasonable to us that B(C$_6$F$_5$)$_3$ binding could lead to an amplification effect, where interaction with a single PT site would impact the optical properties of several PT-CDT repeat units. To examine this possibility we re-examined in more detail the interaction between oligomer **8** and
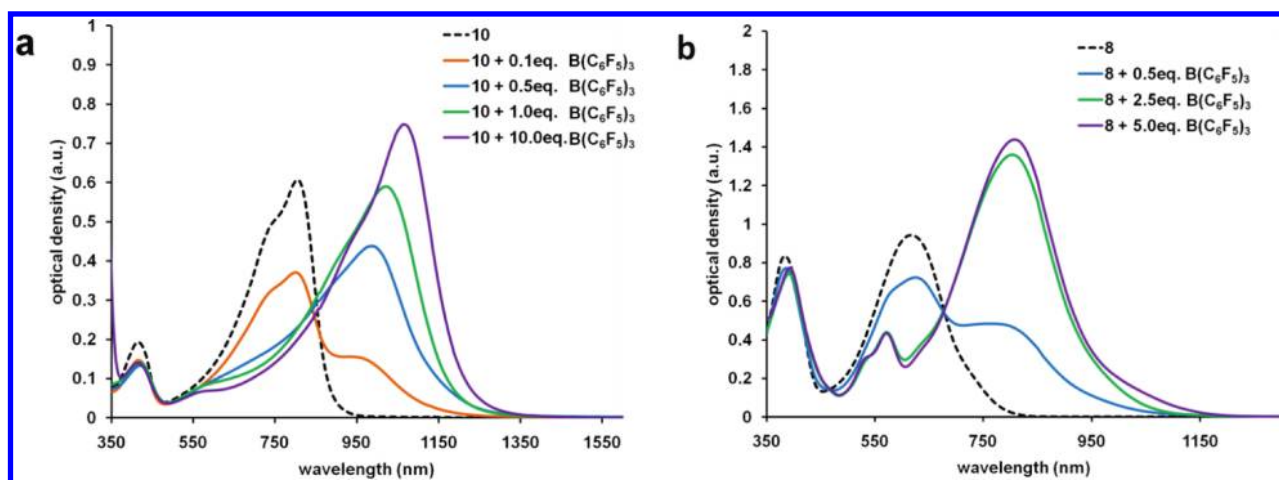
H

dx.doi.org/10.1021/ja110968m |*J. Am. Chem. Soc.* XXXX, XXX, 000–000

Figure 9. UV−vis−NIR absorption spectra of polymer **10** (a) and oligomer **8** (b) with varying equivalents of $B(C_6F_5)_3$ in o-DCB at room temperature under N_2.
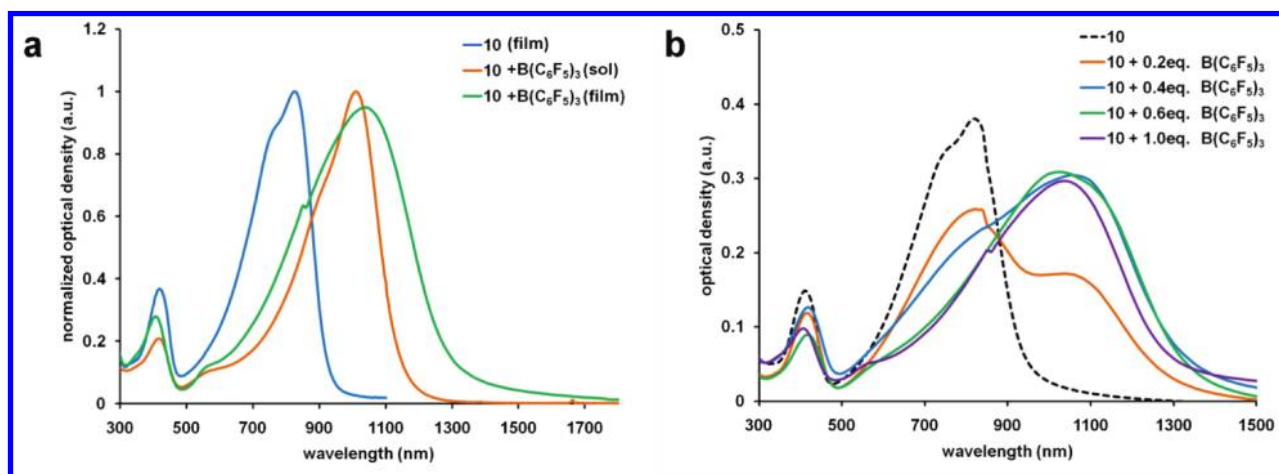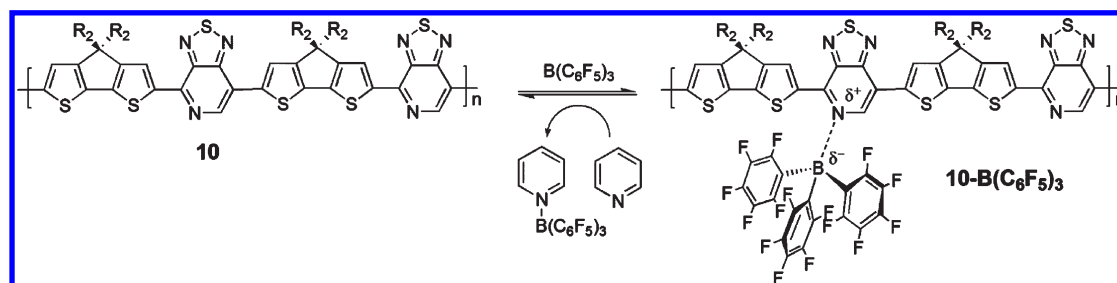

Figure 10. Normalized UV−vis−NIR absorption spectra of (a) **10** with 1 equiv $B(C_6F_5)_3$ in o-DCB solution at room temperature under N_2 (orange), with 1 equiv $B(C_6F_5)_3$ as thin films (green). (b) Absorption spectra of **10** plus varying equivalents of $B(C_6F_5)_3$ as thin films on quartz cast from CB at 1500 rpm under an N_2 atmosphere.

$B(C_6F_5)_3$, see Figure 9b. By looking at the change in absorbance upon addition of 0.5 equiv of $B(C_6F_5)_3$, one can estimate that approximately 25% of **8** is bound, while increasing the concentration to 2.5 equiv shifts the equilibrium toward nearly quantitative adduct formation. Further addition, up to 5 equiv, has minimal impact on the optical absorption spectrum. If one assumes a similar binding constant for **10**, then one-quarter of the PT fragments in the polymer should be bound under similar conditions. This assumption is reasonable given the similar basicity and local steric environment of the PT units in **8** and **10**. In fact, it would not be surprising if the binding constant for **10** is smaller given the more restricted environment within the macromolecular framework and the fact that attaching one $B(C_6F_5)_3$ unit leads to a net decrease in electron density on the backbone. We can thus conclude that only a fractional number of PT units (25% or less) in **10** are occupied upon addition of 0.5 equiv of $B(C_6F_5)_3$, and that this structural modification completely modifies the intrinsic absorption features of the entire polymer chain. Beyond this point, when additional Lewis acid is introduced, there is a further increase in the number of bound PT units, leading to the further red shift

in absorbance shown in Figure 9a. *Therefore, there is an amplification effect of Lewis acid binding to a conjugated polymer backbone that is not readily achieved with small molecule counterparts.*

Transitioning from solution to thin film, a red shift of 52 and 128 nm is observed for the λ_{max} and λ_{onset} of **10**−$B(C_6F_5)_3$ (Figure 10a, Table 2), a possible result of closer interpolymer chain interactions and the anticipated shift toward B−N adduct formation. It is noteworthy that, upon addition of $B(C_6F_5)_3$ to **10**, a red shift of ∼340 nm in the thin film absorption onset, compared to parent spectrum of **10**, can be achieved. Investigation of the binding of $B(C_6F_5)_3$ to **10** in the solid state (Figure 10b) revealed no further changes after addition of approximately 0.6 equiv of Lewis acid, which suggests that binding saturates after (on average) every second PT unit has been coordinated (Scheme 6). Furthermore, we suggest that the additional encumbrance by the borane should suppress interchain S···N interactions that can mediate solid state organization.[67,68]

In a similar fashion, the **11**−$B(C_6F_5)_3$ adduct can be readily obtained upon addition of $B(C_6F_5)_3$ to **11**. The optical absorption spectra in solution and as thin films are shown in Figure 11

I

dx.doi.org/10.1021/ja110968m |*J. Am. Chem. Soc.* XXXX, XXX, 000–000

Scheme 6. Proposed Interaction between Polymer 10 and $B(C_6F_5)_3$[a]

[a] On the basis of optical absorption saturation studies in the solid state, only half of the PT acceptor units can interact with $B(C_6F_5)_3$. Adduct formation is fully reversible in the presence of Py. R_2 = 2-ethylhexyl.
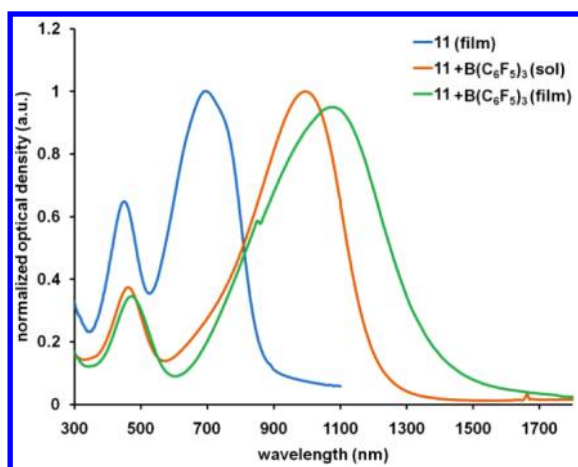

Figure 11. Normalized UV–vis–NIR absorption spectra of **11** as thin films (blue), with 1 equiv $B(C_6F_5)_3$ in o-DCB solution at room temperature under N_2 (orange), with 1 equiv $B(C_6F_5)_3$ as thin films (green).

and are summarized in Table 2. The $11-B(C_6F_5)_3$ adduct has significant absorption into the NIR-region with λ_{onset} values in solution and the solid state of 1236 and 1395 nm, respectively. Compared to $10-B(C_6F_5)_3$, $11-B(C_6F_5)_3$ has a smaller optical band gap, which we attribute to a stronger B–N interaction as a result of the additional thiophene linkages, which likely provide a more basic and sterically accessible coordination site for binding $B(C_6F_5)_3$. It is also worth mentioning that, for both polymers, addition of $B(C_6F_5)_3$ only affects the low energy charge transfer energy band, while the high energy band at ~400–450 nm remains virtually unchanged. While the complexation of halogenated main group Lewis acids to rigid-rod poly(p-phenylene-benzobisthiazole) type polymers has been reported,[69−72] no significant changes in the optical properties of the parent polymers were observed. Thus, these findings therefore present a facile method for red-shifting the optical absorption spectra of narrow band gap polymers.

Determination of the Frontier Molecular Orbital Energy Levels and the Impact of $B(C_6F_5)_3$ Coordination. To gain insight into the nature of the electronic states we estimated the HOMO energy levels of each material as thin films using ultraviolet photoemission spectroscopy (UPS). The more typical approach involving electrochemical determination via cyclic voltammetry (CV) experiments was not feasible due to the instability of the $B(C_6F_5)_3$ adducts in typical supporting

Table 3. Summary of HOMO–LUMO Energy Levels Obtained via UPS and Absorption Spectroscopy

compound[a]	HOMO[b]	LUMO[c]	E_g^d	compound	HOMO[b]	LUMO[c]	E_g^d
8	−4.86	−3.29	1.57	10	−5.01	−3.70	1.31
8−$B(C_6F_5)_3$	−5.37	−4.06	1.31	10−$B(C_6F_5)_3$	−5.24	−4.28	0.96
9	−4.79	−3.18	1.61	11	−4.91	−3.49	1.42
9−$B(C_6F_5)_3$	−5.08	−4.00	1.08	11−$B(C_6F_5)_3$	−5.23	−4.34	0.89

[a] Thin films on Au substrates. [b] In electron volts. Obtained from UPS measurements. [c] In electron volts. Estimated by using the UPS-determined HOMO value and the optical band gap (E_g). [d] Estimated from the onset of film absorption.

electrolytes. Table 3 summarizes the UPS results; spectra can be found in the Supporting Information. It is worth pointing out that the HOMO levels determined via UPS for $10-11$ match those obtained by CV to within ~0.1 eV, see Supporting Information. The HOMO energy levels for polymers **10** and **11** were determined to be −5.01 and −4.91 eV, respectively. On the basis of the onset of optical absorption, we estimated the LUMO energy levels at −3.70 and −3.49, for **10** and **11**, respectively. The destabilization of both the HOMO and LUMO of **11** compared to **10** is a result of the increased electron density across the π-conjugated system afforded by the additional two electron rich thiophene moieties per repeat unit. A similar but less pronounced trend can be observed with **8** ($E_{LUMO} = -3.29$ eV) and **9** ($E_{LUMO} = -3.18$ eV).

Interaction of the small molecules and/or polymers with $B(C_6F_5)_3$ results in a synergetic lowering of both the HOMO and LUMO energy levels, with the LUMO exhibiting the greatest change. For example, the HOMO and LUMO energies of polymer **10** were determined to be −5.01 and −3.70 eV, respectively (Table 3). Binding $B(C_6F_5)_3$ to the polymeric backbone via a B–N dative interaction yields the adduct $10-B(C_6F_5)_3$ *vide supra*, which was determined to have HOMO and LUMO energies of −5.24 and −4.28 eV, respectively (Table 3). Here, interaction of the polymer with $B(C_6F_5)_3$ causes a lowering of the HOMO by 0.23 eV while the LUMO is lowered by 0.58 eV. The greater change in the LUMO energy by 0.35 eV results in the narrowing of the optical band gap. These data imply that coordination of $B(C_6F_5)_3$ to the PT acceptor unit not only removes electron density away from this unit, but also from the entire π-conjugated system. Quite remarkably, for each material, the HOMO is lowered in energy by ~0.2–0.5 eV, upon $B(C_6F_5)_3$ coordination, and thus this method of adduct formation presents itself as a facile route toward significantly modifying
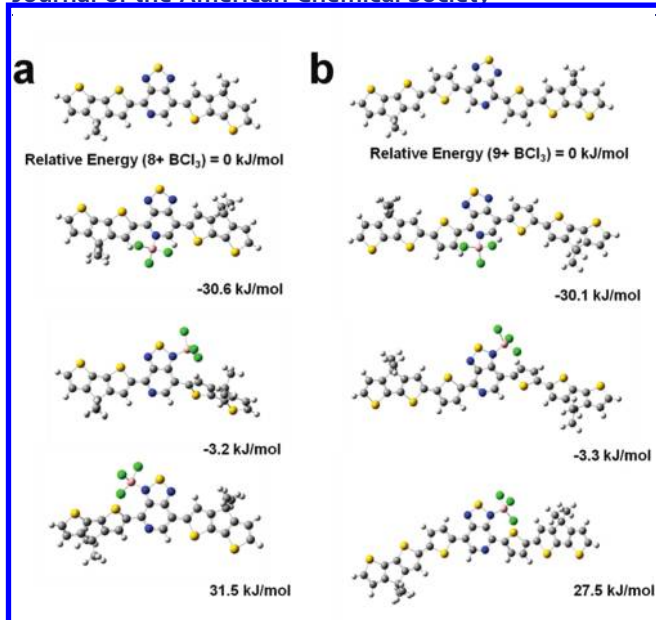
Figure 12. Ground state geometry optimizations of (a) **8** and (b) **9** and their corresponding adducts with BCl_3. Methyl groups were used in place of the hexyl side chains on the dithiophene bridging carbon, while chlorine atoms were used instead of C_6F_5 on boron. Color scheme: carbon, gray; nitrogen, blue; sulfur, orange; boron, pink; chlorine, green. Optimized structures calculated using DFT at the B3LYP/6-31G(d,p) level of theory. Relative energies are shown under each diagram.
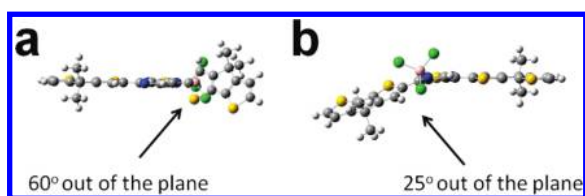

Figure 13. Perspectives of (a) **8**−BCl_3 binding through azole N-atom (left) and (b) **8**-BCl_3 binding through pyridal N-atom (right) that highlight the torsion angle between the CDT and PT units.

both of the HOMO/LUMO energy levels of π-conjugated materials. Comparing polymers **10** to **11**, adduct formation with $B(C_6F_5)_3$ results in a lowering of the HOMO energy levels by 0.23 and 0.32 eV, respectively. It is plausible that the slightly larger change for **11** is due to the increased strength of the acid−base adduct, which is anticipated to be more effective at depleting electron density from the π-conjugated system. Comparing **8** to **9**, adduct formation results in a decrease in the HOMO energy levels by 0.51 and 0.29 eV, respectively. Interestingly, all B-$(C_6F_5)_3$ adducts have LUMO energy levels below −4 eV, which may lend themselves useful as n-type materials in the fabrication of organic solar cells.[73]

Computational Investigation of Regioselective Lewis Acid Coordination and Band Gap Narrowing. Density functional theory (DFT) methods were used to gain insight into the nature of the chromophore−borane interaction. Analogues of **8** and **9** were optimized at the B3LYP/6-31G** level of theory with the simplification of replacing the hexyl chains with methyl groups. Adducts with BCl_3 bound independently to each N-atom of the PT unit were subsequently optimized, see Supporting Information. The Cl atoms, which have a similar electron affinity as the

Table 4. Summary of HOMO and LUMO Energy Level Values Determined by DFT Calculations[a]

compound	HOMO (eV)	LUMO (eV)	E_g (calcd)
8	−4.73	−2.80	1.93
8−BCl_3	−5.17	−3.46	1.71
9	−4.65	−2.86	1.79
9−BCl_3	−4.95	−3.48	1.47

[a] B3LYP/6-31G(d,p).

C_6F_5 aryl rings, were used to enable convergence to a global minimum. Relative energies determined from the optimized structures show that adduct formation at the pyridal N-atom is more favorable by a minimum of 27 kJ/mol over adduct formation at the azole N-atom (Figure 12). The optimized structures also reveal that binding of the borane to one of the azole N-atoms results in a distortion from planarity of a CDT unit by nearly 60°, whereas binding of B to the pyridal N-atom only forces one CDT unit 25° out of plane (Figure 13). These results are consistent with our previous proposal that the more pronounced affinity of the Lewis acidic borane to bind the pyridal N-atom is a consequence of a combination of increased basicity and steric accessibility. Furthermore, it is noteworthy to mention that the distortion from planarity along the π-conjugated backbone upon adduct formation would be anticipated to decrease π-electron conjugation.[71] The observed band gap narrowing implies that the increased electron redistribution afforded by the increase of the electron affinity of the PT acceptor overcompensates for loss in delocalization.

Lewis adduct formation significantly modifies the molecular orbital energy levels. Focusing on **8**, the HOMO and LUMO energy levels were calculated to be −4.73 and −2.80 eV, respectively. With coordinated BCl_3, these energy levels decrease to −5.17 and −3.46, respectively. The changes in absolute energies determined by UPS measurements are in good agreement with these trends. Specifically, *both* the HOMO and LUMO energies decrease in energy upon Lewis acid complexation. However, the LUMO energy level is more affected, consistent with the experimental results in Table 3. Examination of the electron distribution of the HOMO also reveals a slightly greater localization on the CDT units upon Lewis acid binding (Supporting Information).

■ CONCLUSIONS

To summarize, we have shown how to modulate the absorption properties of donor/acceptor conjugated polymers by coordination of Lewis acids to heteroatoms on the acceptor fragments. When examining the widely used polymer **1**, one finds that the driving force for binding $B(C_6F_5)_3$ to the BT azole N-atom is considerably reduced relative to previously examined small molecule analogues. From the reactivity of model compounds **2** (which binds strongly) and **3** (which binds weakly), we surmise that the flanking CDT units adjacent to each BT fragment in **1** provide steric interference that shifts the equilibrium for $B(C_6F_5)_3$ adduct formation toward the unbound species. It is possible to circumvent these steric limitations by using the smaller BBr_3; however, the ensuing adducts are unstable, most likely as a result of propensity for B−Br bond cleavage and bromide generation, and are therefore difficult to properly characterize.

Successful formation of polymer$-$B$(C_6F_5)_3$ adducts required the introduction of the PT subunit as the acceptor segment. Our original thoughts for structural design focused on the more basic and sterically accessible pyridal N-atom, relative to the azole N-atom in BT, as shown in Scheme 3. Indeed, we find that polymer **10** has a greater affinity for B$(C_6F_5)_3$ than **1**, despite their structural similarities. Similar tendencies are observed with the small molecule analogues **8** and **3**. Examination of the differences by which the absorption characteristics of **8** and **10** change with a given quantity of borane shows that there is a previously not observed amplification effect, whereby the binding of B$(C_6F_5)_3$ to a fractional number of basic sites can change the optical properties of the entire backbone. Introduction of electron donating thiophene units adjacent the PT acceptor, specifically the generation of **11** and **9**, has the effect of increasing both the distance between the PT unit and the alkyl side chains and the electron density across the π-conjugated system. The increased electron density, and more open coordination site of the PT unit, results in stronger B$-$N interactions upon Lewis acid adduct formation. One therefore observes larger changes in the optical band gaps of **9** and **11**, compared to **8** and **10**, upon B$(C_6F_5)_3$ coordination. From a materials perspective, it is worth pointing out that, through the binding of B$(C_6F_5)_3$, new NIR-absorbing polymers can be readily generated with band gaps of 0.96 and 0.89 eV, for **10**- B(C_6F_5) and **11**- B(C_6F_5), respectively.

The combination of experimental estimates of HOMO$-$LUMO levels and the DFT results provides additional insights on the role of Lewis acid binding on the preferences for site attachment and the electronic structure of the chromophores. By using BCl$_3$ as the model acid, we find that there is a thermodynamic preference for attaching to the pyridal N-atom over the azole N-atom, consistent with the composite body of experimental results. Coordination of the chromophore to the electron deficient boron results in a lowering of both HOMO and LUMO levels. However, the effect is more pronounced for the LUMO, which resides predominantly near the acceptor fragment. This differential influence over the HOMO and the LUMO is responsible for the observed decrease in band gap energy.

■ ASSOCIATED CONTENT

ⓢ **Supporting Information.** Full details on materials synthesis, spectroscopic characterization, and all computational results. Complete ref 11. This material is available free of charge via the Internet at http://pubs.acs.org.

■ AUTHOR INFORMATION

Corresponding Author
bazan@chem.ucsb.edu

■ ACKNOWLEDGMENT

■ REFERENCES

(1) Forrest, S. R.; Thompson, M. E. *Chem. Rev.* **2007**, *107*, 923–925.

(2) Meier, H. *Angew. Chem., Int. Ed.* **2005**, *44*, 2482–2506.

(3) Karsten, B. P.; Bijleveld, J. C.; Viani, L.; Cornil, J.; Gierschner, J.; Janssen, R. A. J. *J. Mater. Chem.* **2009**, *19*, 5343–5350.

(4) Bijleveld, J. C.; Shahid, M.; Gilot, J.; Wienk, M. M.; Janssen, R. A. J. *Adv. Funct. Mater.* **2009**, *19*, 3262–3270.

(5) Luo, M.; Shadnia, H.; Qian, G.; Du, X. B.; Yu, D. B.; Ma, D. G.; Wright, J. S.; Wang, Z. Y. *Chem.—Eur. J.* **2009**, *15*, 8902–8908.

(6) Hellstrom, S.; Zhang, F. L.; Inganas, O.; Andersson, M. R. *Dalton Trans.* **2009**, 10032–10039.

(7) Zhang, F. L.; Bijleveld, J.; Perzon, E.; Tvingstedt, K.; Barrau, S.; Inganas, O.; Andersson, M. R. *J. Mater. Chem.* **2008**, *18*, 5468–5474.

(8) Beaujuge, P. M.; Ellinger, S.; Reynolds, J. R. *Nat. Mater.* **2008**, *7*, 795–799.

(9) Son, H. J.; Han, W. S.; You, D. H.; Min, K. T.; Kwon, S. N.; Ko, J.; Kang, S. O. *J. Org. Chem.* **2009**, *74*, 3175–3178.

(10) van Mullekom, H. A. M.; Vekemans, J. A. J. M.; Meijer, E. W. *Chem.—Eur. J.* **1998**, *4*, 1235–1243.

(11) Albota, M.;; et al. *Science* **1998**, *281*, 1653–1656.

(12) Entwistle, C. D.; Marder, T. B. *Chem. Mater.* **2004**, *16*, 4574–4585.

(13) Lesley, M. J. G.; Woodward, A.; Taylor, N. J.; Marder, T. B.; Thornton, A.; Bruce, D. W.; Kakkar, A. K. *Chem. Mater.* **1998**, *10*, 1355–1365.

(14) Haldi, A.; Kimyonok, A.; Domercq, B.; Hayden, L. E.; Jones, S. C.; Marder, S. R.; Weck, M.; Kippelen, B. *Adv. Funct. Mater.* **2008**, *18*, 3056–3062.

(15) Chen, C. T. *Chem. Mater.* **2004**, *16*, 4389–4400.

(16) Zeng, W. D.; Cao, Y. M.; Bai, Y.; Wang, Y. H.; Shi, Y. S.; Zhang, M.; Wang, F. F.; Pan, C. Y.; Wang, P. *Chem. Mater.* **2010**, *22*, 1915–1925.

(17) Mishra, A.; Fischer, M. K. R.; Bauerle, P. *Angew. Chem., Int. Ed.* **2009**, *48*, 2474–2499.

(18) Choi, H.; Baik, C.; Kang, S. O.; Ko, J.; Kang, M. S.; Nazeeruddin, M. K.; Gratzel, M. *Angew. Chem., Int. Ed.* **2008**, *47*, 327–330.

(19) Dennler, G.; Scharber, M. C.; Brabec, C. J. *Adv. Mater.* **2009**, *21*, 1323–1338.

(20) Cheng, Y. J.; Yang, S. H.; Hsu, C. S. *Chem. Rev.* **2009**, *109*, 5868–5923.

(21) Kroon, R.; Lenes, M.; Hummelen, J. C.; Blom, P. W. M.; De Boer, B. *Polym. Rev.* **2008**, *48*, 531–582.

(22) Chen, J. W.; Cao, Y. *Acc. Chem. Res.* **2009**, *42*, 1709–1718.

(23) Qian, G.; Wang, Z. Y. *Chem.—Asian J.* **2010**, *5*, 1006–1029.

(24) Gong, X.; Tong, M. H.; Xia, Y. J.; Cai, W. Z.; Moon, J. S.; Cao, Y.; Yu, G.; Shieh, C. L.; Nilsson, B.; Heeger, A. J. *Science* **2009**, *325*, 1665–1667.

(25) Qian, G.; Wang, Z. Y. *Can. J. Chem.* **2010**, *88*, 192–201.

(26) Blouin, N.; Michaud, A.; Gendron, D.; Wakim, S.; Blair, E.; Neagu-Plesu, R.; Belletete, M.; Durocher, G.; Tao, Y.; Leclerc, M. *J. Am. Chem. Soc.* **2008**, *130*, 732–742.

(27) Roncali, J. *Chem. Rev.* **1997**, *97*, 173–205.

(28) Romero-Nieto, C.; Durben, S.; Kormos, I. M.; Baumgartner, T. *Adv. Funct. Mater.* **2009**, *19*, 3625–3631.

(29) Hancock, J. M.; Jenekhe, S. A. *Macromolecules* **2008**, *41*, 6864–6867.

(30) Kappaun, S.; Horner, S.; Kelterer, A. M.; Waich, K.; Grasse, F.; Graf, M.; Romaner, L.; Niedermair, F.; Mullen, K.; Grimsdale, A. C.; Saf, R.; List, E. J. W.; Zojer, E.; Slugovc, C. *Macromol. Chem. Phys.* **2008**, *209*, 2122–2134.

(31) Terashima, T.; Nakashima, T.; Kawai, T. *Org. Lett.* **2007**, *9*, 4195–4198.

(32) Sun, M. T. *J. Chem. Phys.* **2006**, *124*, 054903.

(33) Yasuda, T.; Yamamoto, T. *Macromolecules* **2003**, *36*, 7513–7519.

(34) Monkman, A. P.; Palsson, L. O.; Higgins, R. W. T.; Wang, C. S.; Bryce, M. R.; Batsanov, A. S.; Howard, J. A. K. *J. Am. Chem. Soc.* **2002**, *124*, 6049–6055.

(35) Liaw, D. J.; Wang, K. L.; Chang, F. C. *Macromolecules* **2007**, *40*, 3568–3574.

(36) Yamamoto, T.; Fukumoto, H.; Koizumi, T. *J. Inorg. Organomet. Polym. Mater.* **2009**, *19*, 3–11.

(37) Tolosa, J.; Zucchero, A. J.; Bunz, U. H. F. *J. Am. Chem. Soc.* **2008**, *130*, 6498–6506.

(38) Zucchero, A. J.; Wilson, J. N.; Bunz, U. H. F. *J. Am. Chem. Soc.* **2006**, *128*, 11872–11881.

(39) Wilson, J. N.; Bunz, U. H. F. *J. Am. Chem. Soc.* **2005**, *127*, 4124–4125.

(40) Moliton, A.; Hiorns, R. C. *Polym. Int.* **2004**, *53*, 1397–1412.

(41) Patil, A. O.; Heeger, A. J.; Wudl, F. *Chem. Rev.* **1988**, *88*, 183–200.

(42) Welch, G. C.; Coffin, R.; Peet, J.; Bazan, G. C. *J. Am. Chem. Soc.* **2009**, *131*, 10802–10803.

(43) Job, A.; Wakamiya, A.; Kehr, G.; Erker, G.; Yamaguchi, S. *Org. Lett.* **2011**, *12*, 5470–5473.

(44) Piers, W. E. *Adv. Organomet. Chem.* **2005**, *52*, 1−76.

(45) Erker, G. *Dalton Trans.* **2005**, 1883–1890.

(46) Piers, W. E.; Chivers, T. *Chem. Soc. Rev.* **1997**, *26*, 345–354.

(47) Chen, E. Y. X.; Marks, T. J. *Chem. Rev.* **2000**, *100*, 1391–1434.

(48) Parks, D. J.; Piers, W. E. *J. Am. Chem. Soc.* **1996**, *118*, 9440–9441.

(49) Stephan, D. W.; Erker, G. *Angew. Chem., Int. Ed.* **2010**, *49*, 46–76.

(50) Chase, P. A.; Welch, G. C.; Jurca, T.; Stephan, D. W. *Angew. Chem., Int. Ed.* **2007**, *46*, 8050–8053.

(51) Welch, G. C.; Juan, R. R. S.; Masuda, J. D.; Stephan, D. W. *Science* **2006**, *314*, 1124–1126.

(52) Coffin, R. C.; Peet, J.; Rogers, J.; Bazan, G. C. *Nat. Chem.* **2009**, *1*, 657–661.

(53) Zhu, Z.; Waller, D.; Gaudiana, R.; Morana, M.; Muhlbacher, D.; Scharber, M.; Brabec, C. *Macromolecules* **2007**, *40*, 1981–1986.

(54) Muhlbacher, D.; Scharber, M.; Morana, M.; Zhu, Z. G.; Waller, D.; Gaudiana, R.; Brabec, C. *Adv. Mater.* **2006**, *18*, 2884.

(55) Peet, J.; Kim, J. Y.; Coates, N. E.; Ma, W. L.; Moses, D.; Heeger, A. J.; Bazan, G. C. *Nat. Mater.* **2007**, *6*, 497–500.

(56) Massey, A. G.; Park, A. J. *J. Organomet. Chem.* **1966**, *5*, 218–&.

(57) Focante, F.; Mercandelli, P.; Sironi, A.; Resconi, L. *Coord. Chem. Rev.* **2006**, *250*, 170–188.

(58) Fukumoto, H.; Yamamoto, T. *J. Polym. Sci., Part A: Polym. Chem.* **2008**, *46*, 2975–2982.

(59) Huaxing, Z.; Yang, L.; Price, S. C.; Knight, K. J.; You, W. *Angew. Chem., Int. Ed.* **2010**, *49*, 7922–7995.

(60) Melucci, M.; Favaretto, L.; Zanelli, A.; Cavallini, M.; Bongini, A.; Maccagnani, P.; Ostoja, P.; Derue, G.; Lazzaroni, R.; Barbarella, G. *Adv. Funct. Mater.* **2010**, *20*, 445–452.

(61) Moule, A. J.; Tsami, A.; Buennagel, T. W.; Forster, M.; Kronenberg, N. M.; Scharber, M.; Koppe, M.; Morana, M.; Brabec, C. J.; Meerholz, K.; Scherf, U. *Chem. Mater.* **2008**, *20*, 4045–4050.

(62) Karsten, B. P.; Janssen, R. A. J. *Org. Lett.* **2008**, *10*, 3513–3516.

(63) Geier, S. J.; Stephan, D. W. *J. Am. Chem. Soc.* **2009**, *131*, 3476–3477.

(64) Geier, S. J.; Gille, A. L.; Gilbert, T. M.; Stephan, D. W. *Inorg. Chem.* **2009**, *48*, 10466–10474.

(65) Di Saverio, A.; Focante, F.; Camurati, I.; Resconi, L.; Beringhelli, T.; D'Alfonso, G.; Donghi, D.; Maggioni, D.; Mercandelli, P.; Sironi, A. *Inorg. Chem.* **2005**, *44*, 5030–5041.

(66) Beringhelli, T.; Maggioni, D.; D'Alfonso, G. *Organometallics* **2001**, *20*, 4927–4938.

(67) Naraso; Wudl, F. *Macromolecules* **2008**, *41*, 3169–3174.

(68) Karikomi, M.; Kitamura, C.; Tanaka, S.; Yamashita, Y. *J. Am. Chem. Soc.* **1995**, *117*, 6791–6792.

(69) Roberts, M. F.; Jenekhe, S. A. *Chem. Mater.* **1994**, *6*, 135–145.

(70) Roberts, M. F.; Jenekhe, S. A. *Polymer* **1994**, *35*, 4313–4325.

(71) Roberts, M. F.; Jenekhe, S. A.; Cameron, A.; Mcmillan, M.; Perlstein, J. *Chem. Mater.* **1994**, *6*, 658–670.

(72) Roberts, M. F.; Jenekhe, S. A. *Chem. Mater.* **1993**, *5*, 1744–1754.

(73) Anthony, J. E.; Facchetti, A.; Heeney, M.; Marder, S. R.; Zhan, X. W. *Adv. Mater.* **2010**, *22*, 3876–3892.

M

dx.doi.org/10.1021/ja110968m |*J. Am. Chem. Soc.* XXXX, XXX, 000–000